J. Earth Syst. Sci. (2021)130 228
https://doi.org/10.1007/s12040-021-01724-w

A comparison of atmospheric geochemistry through lichens from volcanic and non-volcanic areas, north Taiwan

Le-Qi Lin[1,2], Hsueh-Yu Lu[1,*], Ju-Lien Pi[1], Tai-Sheng Liou[1], Wen-Fu Chen[3] and Pei-Shan Hsieh[4]

[1]*Department of Earth and Environmental Sciences, National Chung Cheng University, Chiayi, Taiwan.*
[2]*Department of Mechanical and Aerospace Engineering, The State University of New York at Buffalo, Buffalo, NY, USA.*
[3]*Department of Tourism and Management, Chia Nan University of Pharmacy and Science, Tainan, Taiwan.*
[4]*Green Energy and Environment Research Laboratories, Industrial Technology Research Institute, Hsinchu, Taiwan.*
**Corresponding author. e-mail: sheilu@ccu.edu.tw*

MS received 12 April 2021; revised 30 June 2021; accepted 5 July 2021

Lichens are abundant with functional groups that are capable of adsorbing dissolved metals in moisture and intercepting suspended particles in the atmosphere. Using lichen chemistry as an indicator is a prominent method of assessing a long-term baseline of atmospheric quality. This study collected foliose lichens, *Parmelia* sp., from an area with intensive post-volcanic activity (Tatun Volcano Group) and a deep mountain trail (Nan-ao Trail) in northern Taiwan. The geochemical results show that the lichens from Nan-ao have much higher enrichment factors (EFs) for most metals than those from the Tatun Volcano Group, which revealed that the geochemistry of Nan-ao lichens is dominated by interception of suspended particles rather than absorption of lichen surface. In addition, the fact that no Eu-negative anomaly ($Eu/Eu^* \approx 1.0$) can be observed in the normalized patterns of rare earth elements of lichens from Nan-ao reconfirms the derivation. In contrast, lichens from the Tatun Volcano Group are characterized by lower enrichment factors of metals, evident from Ce-negative and Eu-positive anomalies ($Ce/Ce^* < 0.6$ and $Eu/Eu^* > 1.0$), which implies that the lichen chemistry may be principally established by the chemical adsorption of functional groups on the lichen surface. In addition, the extraordinary enrichment factors of Ca, Mg, Na, and K of lichens near the northern coast ($EF > 10$) prove the involvement of seawater aerosol on the atmospheric chemistry. The lead isotopic compositions reveal that unleaded gasoline could be the dominant source of lead for Nan-ao lichens ($^{207}Pb/^{206}Pb > 0.86$ and $^{208}Pb/^{206}Pb < 2.105$), while the local andesite provides the lead to lichens from the Tatun Volcano Group. However, the Tatun Volcano Group is very close to Taipei City, with all kinds of anthropogenic activities, which also contribute a considerable amount of lead to the atmosphere.

Keywords. Northern Taiwan; lichens as bioindicators; rare earth elements; lead isotopes.

Published online: 06 November 2021

1. Introduction

In Taiwan, atmosphere quality is predominantly monitored with the analysis of atmospheric aerosols, including liquid and/or suspended solid particles, collected by air filters and deposition collectors, which demonstrate reliability and efficiency for detecting atmospheric pollution events. However, for a long-term investigation of atmospheric geochemical background like this study, a longer sampling time is necessary to obtain a long-term average. The sampling duration in the range of days to a couple of weeks is not enough for this kind of study (Rossbach *et al.* 1999; Francová *et al.* 2017; Fabri-Jr *et al.* 2018; Kousehlar and Widom 2020). In addition, atmospheric conditions, such as wind, rain, and humidity, can have dramatic effects that complicate the processes of sampling aerosols in a relatively short duration. The collected samples may not represent the typical atmospheric geochemistry, and more weather parameters should be simultaneously measured to adjust the results. Otherwise, a sampling network with a large number of sampling sites should be established to increase the spatial coverage for obtaining a regional average. However, there are some solutions proposed to tackle the difficulties of long-duration sampling and interference of ambient environments (Sahu *et al.* 2011; Sinha *et al.* 2019) and biomonitoring with lichen is just one of the possibilities.

Compared to conventional air sampling techniques, lichens can be efficiently collected without any installation of field equipment. They have been widely used as biomonitors not only at polluted locations for monitoring atmospheric pollution, but also in unpolluted areas for the investigation of regional geochemical backgrounds (Chettri *et al.* 1997; Getty *et al.* 1999; Conti and Cecchetti 2001; Bergamaschi *et al.* 2004; LeGalley *et al.* 2013; Mezhibor *et al.* 2016; Bolshunova *et al.* 2018; Ndlovu *et al.* 2019). The advantage of using lichens as air pollution indicators is made evident in the fact that, lichens are absent of a protective cuticle and well-developed roots, and they subsequently rely on nutrient supply exclusively from the atmosphere (Brown 1976). In addition, the growth rate of lichens is much slower than other plants, and the self-sustaining symbiosis can potentially extend the life span of lichens to decades, sometimes even hundreds to thousands of years in nature (Aubert *et al.* 2006). Therefore, the geochemistry of lichens preferentially represents a long-term average of atmospheric quality. If historical lichen samples were available, the change of atmospheric conditions could also be evaluated (Purvis *et al.* 2007).

In addition to lichen use in air pollution monitoring, there have been many studies demonstrating that lichen geochemistry, which is highly related to their growth environment can serve other purposes, such as exploiting economic ores and monitoring volcanic activities (e.g., Varrica *et al.* 2000). Lichens growing in these areas would accumulate anomalous concentrations of heavy metals.

In recent years, many countries have routinely collected the geochemistry of lichens as an indicator for the investigation of regional geochemical backgrounds (e.g., Getty *et al.* 1999; Rossbach *et al.* 1999; Bergamaschi *et al.* 2004; Koz *et al.* 2010; Will-Wolf *et al.* 2020). Accordingly, this research aims to evaluate the effect on air quality from post-volcanic activity in the Tatun Volcano Group in north Taiwan, and hopefully, it can promote a nationwide project to investigate atmospheric geochemistry using lichens in the near future.

To reveal the source of heavy metals accumulated in lichens, rare earth elements (REEs) were also analyzed in this study. REEs are a suite of 14 metals from atomic number 57 (La) to 71 (Lu), which share similar chemical and physical properties; however, a systematic biogeochemical fractionation, called lanthanide contraction, could occur among REEs due to a gradual change of atomic number (Nesbitt 1979). Accordingly, they have been widely used as a natural tracer or an indicator of redox reaction (e.g., Seto and Akagi 2008; Stille *et al.* 2009; Göb *et al.* 2013; Vázquez-Ortega *et al.* 2015). The major sources of REEs in the atmosphere are marine aerosols and suspended particles of weathered silicate minerals. The REE concentrations of marine aerosols are generally much lower than those of weathered rock dust. During transportation in the atmosphere and/or accumulation in lichens, many processes may modify the concentrations of REEs, which may not be sensitive for identifying the source. However, each source of REEs usually has its unique distribution pattern. A flat pattern could be obtained, if the REE concentrations of lichens were normalized by those of potential source.

In addition to REEs, lead isotopes can be a reliable tracer for indicating both anthropogenic and natural sources due to their greater variability

of isotopic ratios and insignificant fractionation during geological processes. Naturally-occurring lead is composed of four major stable isotopes: ^{204}Pb (1.4%), ^{206}Pb (24.1%), ^{207}Pb (22.1%), and ^{208}Pb (52.10%). Except for the non-radiogenic ^{204}Pb, the other three isotopes are generated from the decay chains of ^{238}U, ^{235}U, and ^{232}Th, respectively (Veron *et al.* 1994; Komárek *et al.* 2008). The atmospheric Pb is normally characterized by different proportions among geological materials from local and/or remote areas and anthropogenic emissions. Accordingly, with the long-term accumulation of heavy metals in lichens, the lead isotopes can effectively indicate the most dominant source of heavy metal in an area.

It is worth mentioning that, biomonitoring with lichen is not a replacement for other sampling methods. There are many disadvantages to monitor atmospheric quality with lichen. One of the critical issues is the selective adsorption of functional groups on lichen surface as the consequence of bioavailability and pH (Purvis and Pawlik-Skowrońska 2008). The selective adsorption would result in fractionation among metals and leads to inconsistency with the results by air filters and deposition collectors. However, lichen still has great performance for long-term monitoring programs and provides information of atmospheric geochemical background. This study is the first attempt in Taiwan to examine the lichens with complete geochemical analysis. The geochemical relationship between lichen and ambient natural environments is the major target in this study. With the results of this study, the geochemical properties of lichen as a proxy of atmospheric geochemical background can be preliminarily revealed and the subsequent monitoring program can be scheduled in the future.

2. Study area

The study area, the Tatun Volcano Group (TVG), is located at the northern tip of Taiwan, only 15 km away from downtown Taipei City (figure 1). It is composed of more than 20 dormant andesitic volcanoes over an area of approximately 150 km^2. The most recent eruption with lava flow was dated at 200,000 years ago, but the deposition of young (<10,000 years ago) volcanic ash can be frequently found in the formations under Taipei City. In addition, according to the study of seismic waves, a deep magma reservoir beneath the Taipei metropolis can be identified (Lin 2016). However, although it is still controversial whether the TVG is active, the extensive emission of fumarolic gases and geothermal springs can be observed in the study area. The top four emission centers are shown in figure 1. These post-volcanic activities introduce large amounts of sulfate into the atmosphere and result in acidic precipitation (Lu 2014). Subsequently, the environment is not favourable for the growth of lichens, and the biodiversity of lichens is actually limited in the study area.

Lichens from a remote area, Nan-ao, were also collected and analyzed for comparison purposes. Nan-ao is also located in northern Taiwan (figure 1). The lichens in Nan-ao were sampled because Nan-ao is situated in a deep mountain area. The sampling locations in Nan-ao can be accessed only by walking, and there is no potential anthropogenic pollution source within the range of 10 km. The lichens can represent the local atmospheric geochemical background. In addition, the distance between Nan-ao and TVG is only about 80 km (figure 1). Both areas share a very similar climate type. The mean annual rainfalls of TVG and Nan-ao are approximately 3000 mm/year. Typhoon events bring in massive precipitation in summer. In winter, the northeast monsoon carries moisture into northern Taiwan and results in continuous precipitation, although the average depth of seasonal precipitation is only about half of the rain in summer. In addition, the elevation of the sampling location in Nan-ao is about 500 m higher than that in TVG. A lower atmospheric temperature can be expected in Nan-ao. These climatic factors may cause different growth rates of lichens, which means that the accumulation time may vary even though lichens are in the same size. It is believed that the concentrations of metals in lichens are highly dependent on accumulation time. Therefore, in this study, the geochemical comparison of lichens from the two areas is based on relative concentrations (enrichment factors) rather than absolute ones as many previous studies did (e.g., Paoli *et al.* 2018; Parviainen *et al.* 2019).

3. Sampling and analytical methods

3.1 *Lichen sampling*

Lichens can be categorized into three main morphological groups: crustose, foliose, and fruticose types (Nash 2008). Crustose lichens are capable of

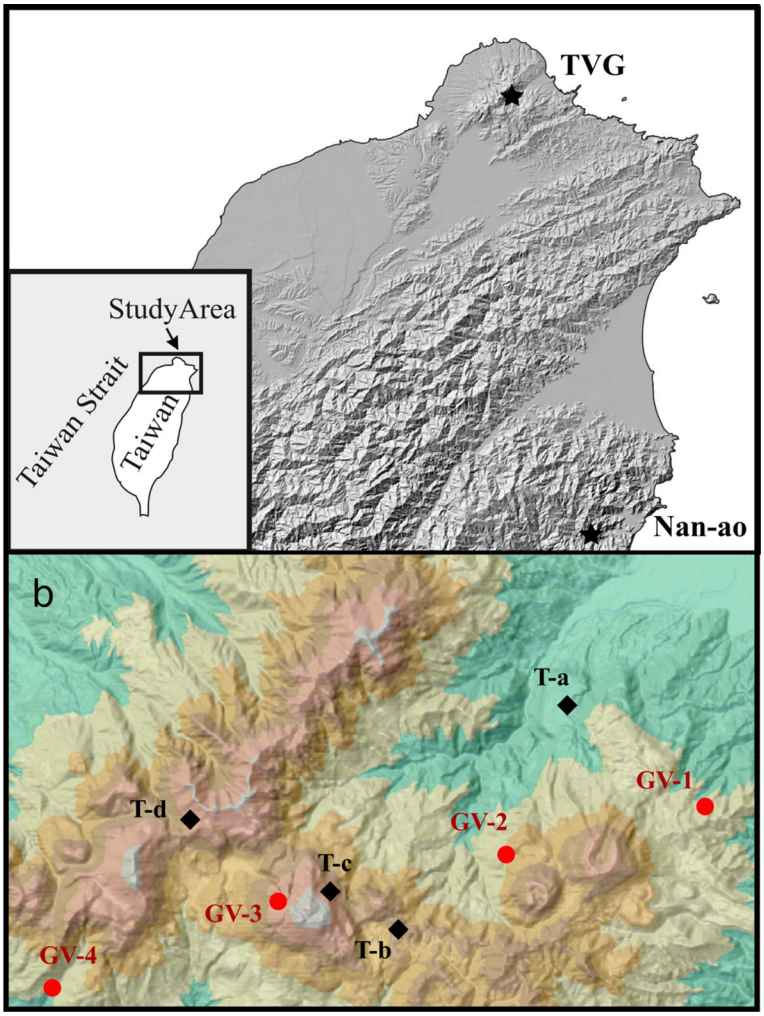

Figure 1. (**a**) Topographic map of northern Taiwan showing the two sampled localities (TVG and Nan-ao). (**b**) Topographic map of the TVG showing sampling sites (T) and major gas vents (GV).

surviving in highly polluted and extreme environments. In contrast, the growth of foliose and fruticose lichens is very sensitive to atmospheric quality, especially the concentrations of sulfur, nitrogen, and fluorine-containing pollutants in air (Nash and Gries 2002; Atari *et al.* 2008; Gibson *et al.* 2013). This study provides evidence that very few lichen species can be found due to post-volcanic activity in the TVG, and most of them belong to crustose families, such as *Lepraria* sp., *Lecanora* sp., *Pertusaria* sp., and *Graphis* sp. However, crustose lichens generally adhere firmly to rocks or trees. It is difficult to separate crustose lichens clearly from substrate and the contamination of substrate would be a serious problem. In addition, it is hard to find fruticose lichen in the TVG. Accordingly, the foliose lichen *Parmelia* sp., which is very common in both areas of the TVG and Nan-ao, was chosen for the geochemical analyses in this study. With identical lichen species, the differences in biogeochemical behaviours can be minimized. In this study, the lichens were collected exclusively from tree bark, and those at a higher distance from the ground were preferred to reduce the interference from ground dust. The sampling locations are shown in figure 1.

3.2 *Sample preparation and chemical analysis*

In the laboratory, the sampled lichens were cut from the tree bark with a ceramic knife, and the extraneous material, such as dead tissue, soil, rock fragments, and tree bark on lichens was carefully removed under a binocular microscope. To ensure that no dust and unwanted material remained on the lichen surface, the lichens were repeatedly cleaned up with an ultrasonic bath. The cleaned samples were dried at 60°C and then ashed in

Pyrex tubes for 4–5 h at 500°C. The ash powder was digested in a mixture of 6 mL ultrapure 6 mL HCl–HNO_3 at 95°C for 1 h (Demiray *et al.* 2012). The digestion solution was finally diluted to 20 mL with deionized water and analyzed for metals by induced coupled plasma-mass spectroscopy (Agilent ICP-MS 7500 cx). To minimize the polyatomic interference of oxides, the ICP-MS was carefully tuned with different sample depths, voltages of the ion lens system, torch temperatures, and helium flow rates in a collision/reaction cell.

3.3 *Data processing*

As stated above, even though lichens grow in the same location, the metal concentrations of lichens may still be related to many factors, especially accumulation time. In addition, although the procedures of sample preparation were identical, the metal concentrations may still be dependent on the water and carbon contents of lichens. To minimize the fluctuations of absolute concentrations, the original measured concentrations can be normalized to the metal concentrations of a chosen reference. It is generally aluminium or titanium to represent the content of clay mineral, which can be one of the potential major sources of atmospheric chemistry (Chiarenzelli *et al.* 2001; Bergamaschi *et al.* 2002; Purvis *et al.* 2007; Agnan *et al.* 2015). However, the concentration of titanium is low and difficult to be measured accurately. In this study, the metal concentrations of lichen samples are normalized by aluminium concentrations themselves to mitigate the effect of accumulation time and then the enrichment factors (EFs) are calculated compared to the earth's upper continental crust (UCC) as the following formula (e.g., Prudêncio 2007; Agnan *et al.* 2014, 2015):

$$\mathrm{EF_M} = \frac{[\mathrm{M/Al}]_{\mathrm{lichen}}}{[\mathrm{M/Al}]_{\mathrm{UCC}}}, \quad (1)$$

where $\mathrm{EF_M}$ is the enrichment factor of metal M; and $[\mathrm{M/Al}]_{\mathrm{lichen}}$ and $[\mathrm{M/Al}]_{\mathrm{UCC}}$ are the ratios of concentration of metal M to aluminum in the lichen and reference UCC, respectively (Taylor and McLennan 1985).

In addition, multivariate statistical analysis is an effective way to elucidate geochemical data. In this study, principal component analysis (PCA) was utilized to depict the geochemical properties of lichens from two sampling areas. PCA is a technique to convert a set of possibly correlated variables into a set of values of independent variables, called principal components (PCs). In the application of lichen geochemistry, PCs generally represent the major source of lichen chemical compositions (e.g., Loppi and Pirintsos 2003; Leonardo *et al.* 2011; Gandois *et al.* 2014). Using PCA in this study, a mixing model of geochemical background in the TVG might be established.

4. Results and discussion

4.1 *Lichen geochemistry*

A total of 11 lichen samples were collected from four sites in the TVG (figure 1). In Nan-ao, four lichens were sampled within a distance of 15 km along the deep mountain trail (figure 1). The samples are labelled according to the following example: for sample T-a-1, T = TVG (if 'T' is replaced by 'N', the samples were collected from the Nan-ao area), a = sampling site and 1 = sample number at the same site. The statistical values of the maximum, minimum, and average chemical compositions for the two areas are summarized in table 1, which can roughly reveal the regional chemical variations of lichens.

In general, the EFs of most metals are relatively depleted in the TVG. It is worth noting that the chemical properties of lichens in Site T-a are quite different from the others in TVG. Compared to lichens from the other TVG sites, those from Site T-a have higher EF values of Na, Mg, K, and Ca, but there is no considerable difference in heavy metals of Fe, Co, Ni, As, and V. On the other hand, the lichens from Nan-ao (Sample N-a) are much enriched in most of the metals, as listed in table 1. The EF values are generally greater than 10, especially for Ca, Mg, Na, and K. The depleted metals (the average of EFs < 1) only include Fe, V, and U. However, Co and Ni are relatively enriched, which is not consistent with the lichens from T-a.

When comparing the lichens from Nan-ao (Site N-a) and TVG (Site T-b to T-d), the differences of alkali and alkali earth elements (Na, K, Ca, Mg, and Sr), transitional metals (Cr, Fe, Co, and Ni) and REEs (La to Lu) can be seen clearly in figure 2. As listed in table 2, the prevailing wind directions (NNW and NW) are not preferred to carry seawater aerosol from the NE coast. Accordingly, the seawater aerosol may not be the source of alkali and alkali earth elements. It is worth noting that

Table 1. *Variations of EFs of lichen metals with basic statistical information.*

T-a ($n = 3$)	Na	Mg	K	Ca	Mn	Fe	Sr	V	Cr	Co
Max.	12.26	70.29	2167.31	24.53	4.76	0.16	3.28	0.33	0.13	0.80
Min.	1.96	21.24	713.53	10.87	2.59	0.02	1.72	0.31	0.07	0.32
Average	6.71	51.44	1456.49	19.30	3.69	0.10	2.43	0.32	0.10	0.55
Range (%)	63.20	41.94	40.78	31.19	24.02	57.87	26.44	1.75	22.23	36.04
T-a ($n = 3$)	Ni	Cu	Zn	As	Ba	Pb	U	La	Sm	Lu
Max.	1.27	63.01	64.35	7.94	13.80	17.57	0.46	0.002	0.002	0.009
Min.	0.57	28.92	39.87	4.23	6.79	9.97	0.17	0.001	0.001	0.002
Average	0.82	49.07	50.08	6.01	10.10	14.00	0.27	0.001	0.001	0.005
Range (%)	38.28	29.73	20.76	25.28	28.48	22.27	49.28	44.10	42.41	56.27
T-b ($n = 2$)	Na	Mg	K	Ca	Mn	Fe	Sr	V	Cr	Co
Max.	0.11	1.86	4.55	0.18	2.51	0.46	1.50	2.65	0.35	0.077
Min.	0.10	1.38	2.99	0.17	2.28	0.38	1.35	2.53	0.30	0.002
Average	0.10	1.62	3.77	0.18	2.39	0.42	1.42	2.59	0.32	0.040
Range (%)	1.67	14.99	20.70	2.67	4.86	9.83	5.31	2.42	7.13	93.73
T-b ($n = 2$)	Ni	Cu	Zn	As	Ba	Pb	U	La	Sm	Lu
Max.	0.84	15.52	159.44	26.96	0.23	325.82	5.74	0.001	0.006	0.004
Min.	0.69	13.53	149.04	26.87	0.21	313.37	4.72	0.001	0.005	0.003
Average	0.76	14.52	154.24	26.92	0.22	319.60	5.23	0.001	0.006	0.004
Range (%)	9.98	6.83	3.37	0.16	5.71	1.95	9.73	1.64	3.25	10.80
T-c ($n = 5$)	Na	Mg	K	Ca	Mn	Fe	Sr	V	Cr	Co
Max.	0.41	1.49	4.90	2.17	6.93	0.58	8.85	2.48	0.11	0.035
Min.	0.07	0.24	0.95	0.15	3.05	0.12	2.53	0.62	0.06	0.001
Average	0.19	0.81	2.85	0.99	4.92	0.31	5.51	1.57	0.09	0.009
Range (%)[a]	67.40	56.59	45.04	81.30	29.78	54.49	47.34	48.95	21.82	138.35
T-c ($n = 5$)	Ni	Cu	Zn	As	Ba	Pb	U	La	Sm	Lu
Max.	1.54	19.64	44.87	39.18	1.41	966.13	2.92	0.003	0.007	0.005
Min.	0.19	5.49	24.39	8.78	0.20	50.30	1.31	0.001	0.001	0.002
Average	0.78	11.13	32.72	23.18	0.76	464.74	2.26	0.002	0.004	0.003
Range (%)[a]	68.12	42.61	21.69	50.87	62.73	85.43	24.30	34.66	53.97	38.18
T-d ($n = 1$)[b]	Na	Mg	K	Ca	Mn	Fe	Sr	V	Cr	Co
Max.	–	–	–	–	–	–	–	–	–	–
Min.	–	–	–	–	–	–	–	–	–	–
Average	0.08	0.29	0.54	0.16	4.07	0.59	2.86	1.47	0.10	0.269
Range (%)[a]	–	–	–	–	–	–	–	–	–	–
T-d ($n = 1$)[b]	Ni	Cu	Zn	As	Ba	Pb	U	La	Sm	Lu
Max.	–	–	–	–	–	–	–	–	–	–
Min.	–	–	–	–	–	–	–	–	–	–
Average	0.49	8.91	50.41	21.18	0.29	62.41	4.22	0.001	0.005	0.007
Range (%)	–	–	–	–	–	–	–	–	–	–
N-a ($n = 4$)	Na	Mg	K	Ca	Mn	Fe	Sr	V	Cr	Co
Max.	32.02	79.96	611.70	610.14	6.79	1.31	18.66	0.68	4.93	6.67
Min.	2.89	42.67	136.28	410.57	2.54	0.49	13.92	0.35	0.98	2.00
Average	13.43	63.90	311.88	519.64	4.17	0.96	15.94	0.48	2.39	4.54
Range (%)[a]	11.62	15.86	183.36	82.01	1.63	0.34	1.86	0.12	1.51	2.11
N-a ($n = 4$)	Ni	Cu	Zn	As	Ba	Pb	U	La	Sm	Lu
Max.	11.05	86.73	38.25	5.04	5.49	10.23	1.29	1.40	3.02	17.38
Min.	3.84	12.34	13.07	2.37	1.50	6.56	0.30	0.86	1.99	1.88
Average	6.56	43.82	21.12	3.60	3.31	8.31	0.63	1.13	2.60	5.97
Range (%)[a]	2.80	27.03	10.10	0.96	1.57	1.44	0.40	0.20	0.42	6.59

[a]Range is calculated by (standard deviation)/average in %.

[b]Only one lichen sample is available. The EFs are shown in average.

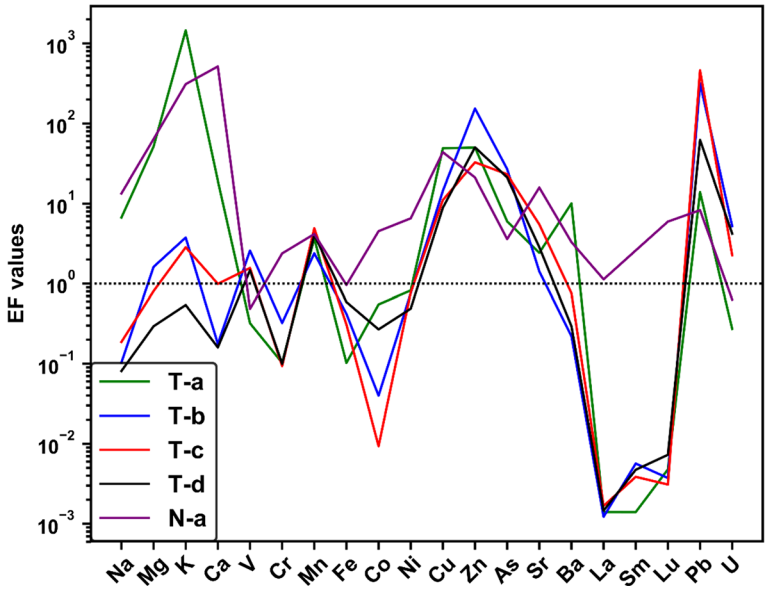

Figure 2. Average EFs of the lichens from each sampling site with the order of atomic number.

Table 2. *Selected geographical and climatic information of sampling locations in this study.*

Site	Elevation (m)	Distance to nearest coast (m)	Prevailing wind[a]		2nd most frequent wind[b]	
			Direction	Speed (m/s)	Direction	Speed (m/s)
T-a	580	7400	NE	1–2	NNE	1–2
T-b	760	10,900	NNE	2–3	NE	1–2
T-c	1020	11,500	NNE	2–3	NE	1–2
T-d	870	12,600	ENE	4–5	WSW	5–6
N-a	700–1500	10,000	NNW	2–3	NW	2–3

[a]The most frequent wind direction and speed at the weather station nearest the lichen sampling site over the period 2015–2019.
[b]The wind direction and speed next to the prevailing wind at the same weather station over the same period.
a and b: All the data were retrieved from the website of the Central Weather Bureau, Taiwan (http://e-service.cwb.gov.tw/HistoryDataQuery/index.jsp).

not all of the heavy metals in the lichens from Nan-ao (N-a) have higher EF values than those from the TVG. The transitional metals of Cu and Zn show similar EF values (figure 2). The elements of Fe, Co, and Ni naturally have higher oxidation numbers (+2 and +3) than Cu and Zn (+1 and +2). Theoretically, the metals with higher oxidation numbers could have stronger hydrolysis reaction in water and tend to form insoluble hydroxides, while Cu and Zn prefer to be hydrated with water molecules (Scholz and Kahlert 2015). It is believed that hydroxides of Fe, Co, and Ni are not preferable to transport in oxidizing atmosphere, compared to the more soluble hydrated Zn and Cu.

Accordingly, the relative depleted transitional metals in lichens from the TVG can be possibly explained by the fact that the functional groups on the lichen surface adsorb chemical compositions dissolved in the atmospheric water vapour. In addition to the adsorption of functional groups, the direct capture of suspended particles by the lichens from Nan-ao may be significant in the enrichment of alkali, alkali earth, and transitional metal elements. This derivation can be reconfirmed with the enrichment of REEs, which are also enriched in the lichens from Nan-ao (figure 2).

4.2 *PCA analysis*

In this study, all chemical components listed in table 1 from all sampling sites were considered as variables for PCA. Subsequently, PCA extracted three PCs having eigenvalues of >1.0, accounting for 86.56% of the total variance. The factor coordinates (eigenvectors) of the variables, eigenvalues, percentage of variance, and cumulative percentage

of variance of three PCs (PC-1 to PC-3) are given in table 3. The eigenvalues of PCs are 12.13, 3.17, and 2.01, which account for 60.67, 13.86, and 10.03% of the total variance, respectively. However, there is only one variable (Zn) with a significant loading of >0.7 in PC-3. This suggests that PC-3 can be considered to have only minor geochemical importance and will not be discussed in this study. Accordingly, the original data were projected into the new coordination system of two major PCs (PC-1 and PC-2), as shown in figure 3.

Table 3 shows that PC-1 strongly correlates with most of the chemical components of lichens. It is predominant that the major PC (PC-1) can distinguish the geochemical properties of lichens between the TVG and Nan-ao (dashed line in figure 3b). This trend from Nan-ao to the TVG demonstrates the decrease of EF values of most elements (table 3), which confirms the derivation from EF values of lichen geochemistry. In contrast, the EF values of V, U, and Pb contemporarily increase in the same trend. These elements are generally enriched in most of the volcanic areas; however, their loadings do not show a substantial correlation. Accordingly, PC-1 simply serves as higher EF values for lichens from Nan-ao. Compared to the enrichment of Na, K, Ca, and Mg for the lichens from T-a, the enrichment of almost all elements indicates that the participation of seawater aerosol is suspicious for Nan-ao lichens. Otherwise, a depletion of Fe, Co, Ni, and other transitional metals should be observed.

It is believed that lichens can scavenge chemicals from the atmosphere with two different mechanisms (Conti and Cecchetti 2001; Bergamaschi *et al.* 2004; Purvis and Pawlik-Skowrońska 2008): (1) Lichens capture suspended micro-particles, which may show similar geochemical properties with clay minerals. (2) The functional groups on the lichen surface absorb dissolved ions from air moisture. It is plausible to suggest that the high EFs (the positive end member of PC-1) result from suspended particulates adding considerable amounts of adsorbed ions. In contrast, the negative end member of PC-1 is characterized by depletion of Fe, Co, Ni, and most REEs (table 1 and figure 2), which may probably represent the dominance of the absorption process over the capture of suspended particles due to the lower solubility of heavy metals during the transportation in the atmosphere. However, in the area with volcanic activity, the high emission of SO_2 and H_2S gases would give rise to an acidic environment and promote the dissolution of metals in the atmospheric moisture. This could possibly enhance the adsorption process.

Table 3. *Factor loadings of the variables based on correlations in PCA for lichen chemistry.*

Components	PC-1	PC-2	PC-3
Na	**0.878**	0.068	0.428
Mg	**0.987**	0.035	–0.055
K	0.560	**0.649**	0.233
Ca	**0.972**	–0.159	–0.118
Mn	**0.915**	–0.130	0.192
Fe	0.530	–0.539	–0.472
Sr	**0.949**	–0.223	–0.215
V	–0.552	**–0.719**	0.288
Cr	**0.822**	–0.160	–0.236
Co	**0.968**	–0.099	0.054
Ni	**0.970**	–0.108	0.172
Cu	**0.904**	0.128	0.345
Zn	0.062	–0.350	**0.728**
As	0.428	**–0.796**	–0.258
Ba	**0.732**	0.460	–0.027
Pb	–0.328	–0.574	0.058
U	–0.519	**–0.637**	0.466
La	**0.920**	–0.199	–0.178
Sm	**0.937**	–0.193	–0.152
Lu	**0.781**	0.003	0.531
Eigenvalue	12.13	3.17	2.01
Total variance (%)	60.67	15.86	10.03
Cumulative (%)	60.67	76.53	86.56

Bold indicates a statistically significant loading.

Figure 3(b) shows that PC-2 is capable of effectively separating the lichens from the TVG. The lichens from sites T-b, T-c, and T-d have relatively higher EF values of As, V, and Pb, which are generally enriched in volcanic gas, but these elements are depleted in the lichens from Site T-a. As mentioned above, Site T-a has the privileged conditions (distance and wind direction, as seen in table 2) to receive seawater aerosol. This derivation can be reconfirmed with the distribution of TVG lichens along PC-2.

4.3 *REE chemistry*

REEs were also analyzed in this study to further understand the geochemical exchange between lichens and the atmosphere. To assume that clay mineral is the major potential source of REEs, the analytical results of REEs were normalized by UCC as the calculation of EF values (Taylor and

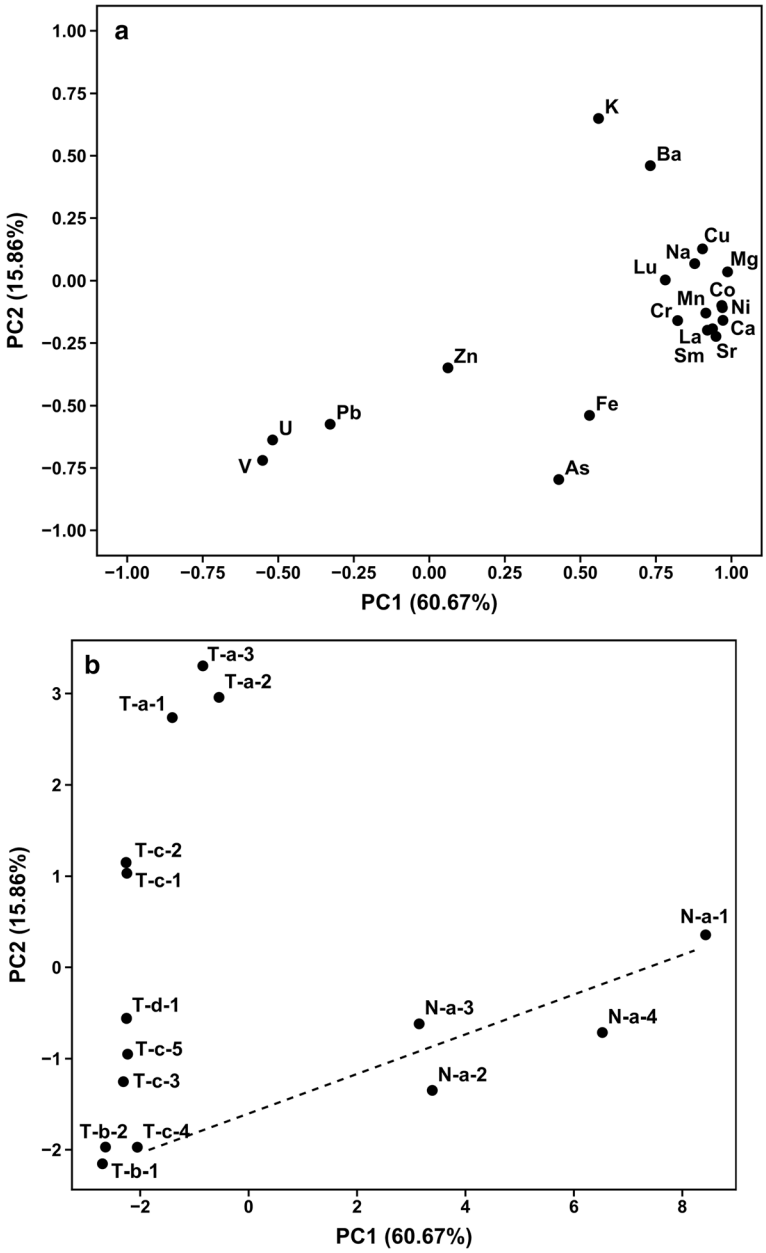

Figure 3. Results of PCA for the lichen chemistry: (**a**) loading plot of PC-1 *vs.* PC-2 and (**b**) projection of chemical components on the plot of PC-1 *vs.* PC-2.

McLennan 1985). In general, the lichens from each site share a similar normalized REE pattern; figure 4 shows the representatives for all sites. There are three distinct types of REE patterns: T-a, T-b to T-d, and N-a. The highest concentrations of REEs are found in the lichens from Nan-ao, which are about 4–20 times those of the TVG (figure 4). The reason for the enrichment of REEs is the same as the EF values, which results from the direct capture of suspended particles on lichen surface. In contrast, the lichens from T-a have much lower concentrations of REEs, as expected, due to the dilution effect of seawater aerosol with very low REE contents.

Most of the REEs naturally have the valency of +3 in the environment, while only cerium (Ce) and europium (Eu) are known to take different valencies of +4 and +2, respectively. The peculiar behaviours of Ce and Eu would accordingly occur due to the difference in ionic charge density, which can be manifested as anomalies in the normalized REE patterns. The anomalies (Ce/Ce^* and Eu/Eu^*) can be quantitatively evaluated with the abundances of neighbouring REEs as equations

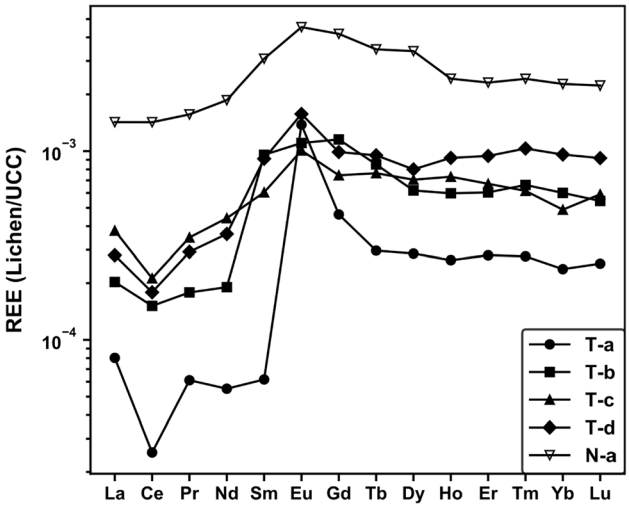

Figure 4. UCC-normalized REE pattern of representative lichens from each sampling site.

(Chiarenzelli *et al.* 2001; Dominique *et al.* 2006; Symphonia and Nathan 2018; Ayala-Pérez *et al.* 2021):

$$(\mathrm{Ce/Ce^*}) = \frac{\mathrm{Ce}}{\sqrt{\mathrm{La} \times \mathrm{Pr}}} \tag{2}$$

$$(\mathrm{Eu/Eu^*}) = \frac{\mathrm{Eu}}{\sqrt{\mathrm{Sm} \times \mathrm{Gd}}}. \tag{3}$$

The calculated results are listed in table 4.

The Ce anomaly is an excellent indicator of redox state. The oxidation environment would result in the dominance of Ce(IV) species, which is preferred to form CeO_2 oxide with very low solubility (Akagi and Masuda 1998). Under this circumstance, it can be expected that the Ce-negative anomaly ($Ce/Ce^* < 1.0$) would be observed, if REEs dissolved in the moisture were transported in the atmosphere. In contrast, the REE pattern of the suspended particles would be preserved during transportation, and there would be no considerable Ce-negative anomaly. Table 4 shows that the Ce-negative anomaly ($Ce/Ce^* < 0.6$) appears in all lichens from the TVG, which demonstrates that the REE origin is dominated by the adsorption process on lichen surface functional groups rather than the direct capture of suspended particles. It is worth noting that the lichens from Site T-a are characterized by the most intense Ce-negative anomaly ($Ce/Ce^* < 0.4$) (table 4 and figure 4). As mentioned, seawater aerosol may make a significant contribution to those near the coastline (Site T-a). It is well recognized that the Ce-negative anomaly extensively appears in seawater due to Ce scavenging by non-dissolved oxide (Piepgras and Jacobsen 1992; Hongo *et al.* 2006; Hathorne *et al.* 2012, 2015; Deng *et al.* 2017). This natural fact reconfirms that the participation of seawater truly affects the geochemical compositions of the lichens from Site T-a. However, although the enrichment of Na, K, Ca, and Mg can also be observed in those from Nan-ao, the inconsiderable Ce-negative anomaly ($Ce/Ce^* > 0.9$) demonstrates that the effect of seawater is negligible.

Table 4. *Geochemical characteristics of REEs for the lichens in this study.*

Sample	Ce/Ce^*	Eu/Eu^*
T-a-1	0.36	8.19
T-a-2	0.35	7.22
T-a-3	0.34	7.02
T-b-1	0.81	1.19
T-b-2	0.80	1.05
T-c-1	0.55	1.40
T-c-2	0.58	1.50
T-c-3	0.61	1.23
T-c-4	0.74	1.33
T-c-5	0.58	1.46
T-d-1	0.62	1.66
N-a-1	0.92	1.99
N-a-2	0.95	1.26
N-a-3	0.93	1.16
N-a-4	0.99	1.24

Eu is traditionally known as a proxy for calcium in plagioclase during igneous fractionation due to its reduced divalent (2+) cation (Weill and Drake 1973). The positive Eu anomaly can be accordingly observed in plagioclase. In this study, the Eu-positive anomaly exists in all lichens from both study areas (table 4), but very strong Eu-positive anomaly occurs only in the lichens from Site T-a ($Eu/Eu^* > 7$) compared to those from all other sites showing minor positive anomaly ($Eu/Eu^* < 2$). Although seawater aerosol is one of the possible sources in Site T-a, the predominant Eu-positive anomaly is rarely observed in open seawater (Olivarez and Owen 1991; Dubinin 2004; Hongo *et al.* 2006; Hathorne *et al.* 2015; Deng *et al.* 2017). Meanwhile, the hydrothermal fluid was frequently reported with highly Eu-positive anomaly due to the strong water–rock interaction, especially in sedimentary host rocks (Olivarez and Owen 1991; Bao *et al.* 2008). According to Wang *et al.* (2004), the TVG andesites demonstrate REE patterns with insignificant negative Eu anomaly. Later studies measured the REE patterns of river water in the TVG watershed, which are also slightly enriched with Eu (Lu 2014; Kao *et al.*

Table 5. *Results of lead isotopic compositions of lichens in this study.*

Lichen	$^{208}Pb/^{206}Pb$	$^{207}Pb/^{206}Pb$	$^{206}Pb/^{204}Pb$
Tatun volcanic group			
T-a-1	2.0974	0.8541	18.2875
T-a-2	2.0954	0.8532	18.3101
T-a-3	2.0961	0.8535	18.2922
T-a-4	2.0968	0.8553	18.2254
T-a-5	2.0945	0.8514	18.3959
T-b-1	2.0948	0.8543	18.2379
T-b-2	2.0940	0.8547	18.3382
T-c-1	2.1015	0.8556	18.2771
T-c-2	2.0990	0.8579	18.2049
T-c-3	2.0982	0.8569	18.2101
T-c-4	2.1019	0.8554	18.2080
T-c-5	2.1002	0.8561	18.1991
T-d-1	2.0995	0.8553	18.2120
Average	2.0976	0.8549	18.2614
Nan-ao			
N-a-1	2.1111	0.8645	18.0765
N-a-2	2.1095	0.8646	18.0847
N-a-3	2.1088	0.8580	18.2310
N-a-4	2.1090	0.8601	18.1801
Average	2.1096	0.8618	18.1431

2017). In this study, the Eu anomalies of lichens, except those from Site T-a, are consistent with those of river water. It is considered that the REEs of hydrothermal fluid in the TVG could be closely associated with those of host andesites. During the weathering process in the hydrothermal system, the plagioclase is likely to be dissolved and provides additional Eu to result in the slight Eu-positive anomaly.

The REE patterns from Site T-a are obviously exceptional ($Eu/Eu^* > 7$) (table 4). As mentioned above, although seawater aerosol can make the lichens at T-a Site show Ce-negative anomaly, it is not possible to depict the extraordinary Eu-positive anomaly with the contribution of seawater aerosol. It is worth noting that there are several minor hydrothermal vents close to Site T-a, which are hosted by sedimentary rocks instead of igneous rocks, as in the other three cases (figure 1). In general, sedimentary rock is highly enriched with plagioclase and can be a substantial source of Eu (Chao *et al.* 2015). It is believed that the plagioclase can be easily dissolved and enhances the Eu-positive anomaly, while the hydrothermal fluid passes through the sedimentary rocks. Although there are no analytical results for the sedimentary rocks from Site T-a, according to unpublished data from the researchers, for the Sr isotopic compositions of hydrothermal fluid, the additional source from sedimentary rocks can be confirmed. The unpublished data reveal that the ratio of $^{87}Sr/^{86}Sr$ of hydrothermal fluid from Site T-a is about 0.714, which is much higher than 0.705 for those from the other sites in the TVG. Because the radioactive decay of ^{87}Rb is one of the major sources of ^{87}Sr, the age of rocks would increase the ratio of $^{87}Sr/^{86}Sr$. And, because the sedimentary rocks are formed by the accumulation of weathered geological material on the Earth's surface, it can be expected that the ratio of $^{87}Sr/^{86}Sr$ of sedimentary rocks must be much higher than those of its parent geological material. Radiometric age dating demonstrates that the TVG is composed of very young andesitic rocks, which have ages from 2.8 to 0.2 Ma and a low ratio of $^{87}Sr/^{86}Sr$, in a range of 0.70414–0.70488 (Wang *et al.* 1999, 2004; Shellnutt *et al.* 2014). Accordingly, the Sr isotopic compositions of hydrothermal fluid at Site T-a actually reveal that the sedimentary source is significant to the hydrothermal fluid at Site T-a, which can support the Eu-positive anomaly observed in the lichens.

4.4 *Lead isotopes*

The analytical results of lead isotopes of lichens demonstrate distinct values from the TVG and Nan-ao. Those from the TVG have lower ratios of $^{208}Pb/^{206}Pb$ and $^{207}Pb/^{206}Pb$ as well as higher ratios of $^{206}Pb/^{204}Pb$ (table 5). However, they still roughly follow a straight-line trend (dashed eclipse in figure 5), which indicates that the lead sources of lichens in this study may be controlled by a mixing model between two major components.

In previous studies, there were some lead isotopes available, including gasoline, suspended particles, and TVG andesite, which can potentially contribute to the lead of lichens in this study. Yao *et al.* (2015) analyzed lead isotopic compositions of unleaded gasoline collected from gas stations in Taipei City. Compared to those in this study, the unleaded gasoline has higher ratios of $^{208}Pb/^{206}Pb$ and $^{207}Pb/^{206}Pb$, but much lower $^{206}Pb/^{204}Pb$ (figure 5). In addition, the lead isotopic compositions published by Wang *et al.* (2004) revealed that local andesites in the TVG have the opposite properties of unleaded gasoline (figure 5). Accordingly, the lichens from the TVG are close to the TVG andesites, and those from Nan-ao lie are nearer to unleaded gasoline. Thus, it is reasonable

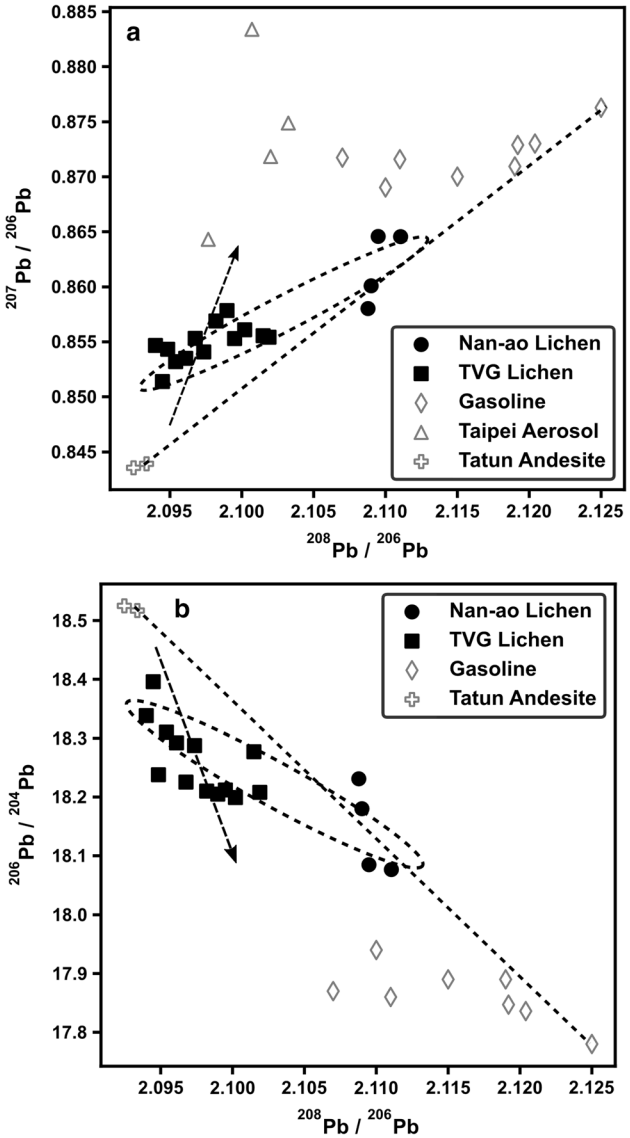

Figure 5. Lead isotopic compositions for the lichens in this study: (**a**) $^{207}Pb/^{206}Pb$ *vs.* $^{208}Pb/^{206}Pb$, (**b**) $^{206}Pb/^{204}Pb$ *vs.* $^{208}Pb/^{206}Pb$.

to expect that the emitted volcanic gases dominate the atmospheric geochemistry around the TVG.

To conceptually connect unleaded gasoline and TVG andesite representing a mixing trend between two-end members (dashed line in figure 5), the lichens from Nan-ao perfectly fall in the mixing line. However, it is unclear, whether TVG andesite can be considered as a major source based on the facts that the two locations are more than 80 km distant (figure 1) and the prevailing wind directions are not preferred to transport volcanic material to Nan-ao (table 2). According to the derivation from the aforementioned results of REEs and general geochemistry, it is believed that sedimentary material contributes significantly to the lichens from Nan-ao. Unfortunately, there are no available data of sedimentary rocks in Taiwan to establish the mixing model between unleaded gasoline and sedimentary rocks. However, the lead isotopic ratios from Nan-ao are akin to those of unleaded gasoline (figure 5), which implies that unleaded gasoline is a major contributor of lead. In contrast, it is surprising that the data points of TVG lichens do not fall within the mixing line, but show some offset towards the higher ratio of $^{207}Pb/^{206}Pb$, which approaches the value of ambient aerosols/suspended particles from Taipei City (dashed arrow in figure 5a). Hsu *et al.* (2006) reported seasonal lead isotopic compositions of $^{208}Pb/^{206}Pb$ and $^{207}Pb/^{206}Pb$ of Taipei City atmospheric aerosols. The authors concluded that the atmospheric aerosols in Taipei City are principally composed of local anthropogenic emission and pollution of long-range transport from southeastern China during the northeast monsoon season. As shown in figure 5(a), the Taipei City aerosols are potentially responsible for the third-end member in addition to the local andesite and unleaded gasoline. Although the ratios of $^{206}Pb/^{204}Pb$ of Taipei City aerosols were absent, the data points of lichens in this study also demonstrate slight deviation from the lower $^{206}Pb/^{204}Pb$, which could possibly represent the lead isotopic compositions of Taipei City atmospheric aerosols (figure 5b). Accordingly, it can be concluded that the lead source of the Tatun atmosphere is dominated by local andesite, but is slightly affected by Taipei City aerosols and unleaded gasoline.

5. Conclusion

This study examines the chemical properties of lichens from a volcanic area (TVG) and undisturbed deep mountain (Nan-ao) to preliminarily understand the long-term baseline of atmospheric geochemistry in northern Taiwan. The results demonstrate that the lichen chemical properties are dominated by two mechanisms, which are the interception of suspended particles and the adsorption of metals on the functional groups of the lichen surface. Lichens can inherit the chemical properties from suspended particles if interception is dominant. On the other hand, the chemical components dissolved in moisture would be fractionated during the processes of transportation in the atmosphere and adsorption on the lichen surface. The lichens from Nan-ao combine both mechanisms to achieve

much higher EFs for most of the metals, while those from the TVG with lower EFs may be mostly affected by the adsorption process. The normalized REE patterns demonstrate that the Ce-negative anomaly commonly exists in most of the lichens from the TVG. It is believed that Ce^{4+} is unlikely to be transported in the atmosphere due to the oxidation environment. The Ce-negative anomaly of lichens also confirms that the chemical properties of TVG lichens are mainly determined by the adsorption process. In addition, the lead isotopes show that TVG lichens were influenced by local andesites, unleaded gasoline, and anthropogenic emissions, while unleaded gasoline is possibly the main source of lead of Nan-ao lichens.

Acknowledgement

This study is supported by research grants from the National Science Council, Taiwan (MOST106-2116-M-194-001-).

Author statement

Le-Qi Lin: Sample preparation, geochemical analysis and contributed to the discussion in the manuscript. Hsueh-Yu Lu: Conceived the idea behind the study, obtained the financial support and manuscript preparation. Ju-Lien Pi: Process design of lead isotopic analysis. The results of lead isotopes are the major parts to explain the sources of atmospheric compositions. Tai-Sheng Liou: Familiar with the atmospheric conditions in north Taiwan and provided valuable information during drafting the manuscript. Wen-Fu Chen: Expert in Tatun Volcano Group and the distribution of volcanic activities in the study area. He also provided valuable information during drafting the manuscript. Pei-Shan Hsieh is familiar with the distribution and geochemical properties of fumarolic gases and geothermal springs in the study area. She provided valuable information during drafting the manuscript.

References

Agnan Y, Séjalon-Delmas N and Probst A 2014 Origin and distribution of rare earth elements in various lichen and moss species over the last century in France; *Sci. Total Environ.* **487** 1–12.

Agnan Y, Séjalon-Delmas N, Claustres A and Probst A 2015 Investigation of spatial and temporal metal atmospheric deposition in France through lichen and moss bioaccumulation over one century; *Sci. Total Environ.* **529** 285–296.

Akagi T and Masuda A 1998 A simple thermodynamic interpretation of Ce anomaly; *Geochem. J.* **32** 301–314.

Atari D O, Luginaah I, Xiaohong X and Fung K 2008 Spatial variability of ambient nitrogen dioxide and sulfur dioxide in Sarnia, 'Chemical Valley' Ontario, Canada; *J. Toxicol. Environ. Part A* **71** 1572–1581.

Aubert D, Le Roux G, Krachler M, Cheburkin A, Kober B, Shotyk W and Stille P 2006 Origin and fluxes of atmospheric REE entering an ombrotrophic peat bog in Black Forest (SW Germany): Evidence from snow, lichens and mosses; *Geochim. Cosmochim. Acta* **70** 2815–2826.

Ayala-Pérez M P, Armstrong-Altrin J S and Machain-Castillo M L 2021 Heavy metal contamination and provenance of sediments recovered at the Grijalva River delta, southern Gulf of Mexico; *J. Earth Syst. Sci.* **130** 88.

Bao S X, Zhou H Y, Peng X T, Ji F W and Yao H Q 2008 Geochemistry of REE and yttrium in hydrothermal fluids from the Endeavour segment, Juan de Fuca Ridge; *Geochem. J.* **42** 359–370.

Bergamaschi L, Rizzio E, Giaveri G, Profumo A, Loppi S and Gallorini M 2004 Determination of baseline element composition of lichens using samples from high elevations; *Chemosphere* **55** 933–939.

Bergamaschi L, Rizzio E, Valcuvia M G, Verza G, Profumo A and Gallorini M 2002 Determination of trace elements and evaluation of their enrichment factors in Himalayan lichens; *Environ. Pollut.* **120** 137–144.

Bolshunova T, Rikhvanov L, Mezhibor A, Zhornyak L, Baranovskaya N and Eremina E 2018 Biogeochemical characteristics of epiphitic lichen *Lobaria pulmonaria* of the Barguzin nature reserve (the republic of Buryatia, Russia); *J. Environ. Eng. Landsc. Manag.* **26** 120–127.

Brown D H 1976 Mineral uptake by lichens; In: *Lichenology: Progress and Problems* (eds) Brown D H, Hawksworth D L and Bailey R H, Academic Press, London, pp. 419–439.

Chao H C, You C F, Liu H C and Chung C H 2015 Evidence for stable Sr isotope fractionation by silicate weathering in a small sedimentary watershed in southwestern Taiwan; *Geochim. Cosmochim. Acta* **165** 324–341.

Chettri M K, Sawidis T and Karataglis S 1997 Lichens as a tool for biogeochemical prospecting; *Ecotoxicol. Environ. Saf.* **38** 322–335.

Chiarenzelli J, Aspler L, Dunn C, Cousens B, Ozarko D and Powis K 2001 Multi-element and rare earth element composition of lichens, mosses, and vascular plants from the Central Barrenlands, Nunavut, Canada; *Appl. Geochem.* **16** 245–270.

Conti M E and Cecchetti G 2001 Biological monitoring: Lichens as bioindicators of air pollution assessment: A review; *Environ. Pollut.* **114** 471–492.

Demiray A D, Yolcubal I, Akyol N H and Çobanoğlu G 2012 Biomonitoring of airborne metals using the Lichen *Xanthoria parietina* in Kocaeli Province, Turkey; *Ecol. Indic.* **18** 632–643.

Deng Y, Ren J, Guo Q, Cao J, Wang H and Liu C 2017 Rare earth element geochemistry characteristics of seawater and

porewater from deep sea in western Pacific; *Sci. Rep.* **7**, https://doi.org/10.1038/s41598-017-16379-1.

Dominique A, Le Roux G, Krachler M, Cheburkin A, Kober B, Shotyk W and Stille P 2006 Origin and fluxes of atmospheric REE entering an ombrotrophic peat bog in Black Forest (SW Germany): Evidence from snow, lichens and mosses; *Geochim. Cosmochim. Acta* **70** 2815–2826.

Dubinin A V 2004 Geochemistry of rare earth elements in the ocean; *Lithol. Miner. Resour.* **39** 289–307.

Fabri-Jr R, Krause M, Dalfior B M, Salles R C, de Freitas A C, da Silva H E, Licinio M V, Brandão G P and Carneiro M T 2018 Trace elements in soil, lichens, and mosses from Fildes Peninsula, Antarctica: Spatial distribution and possible origins; *Environ. Earth Sci.* **77** 124.

Francová A, Chrastný V, Sillerová H, Vítková M, Kocourková J and Komárek M 2017 Evaluating the suitability of different environmental samples for tracing atmospheric pollution in industrial areas; *Environ. Pollut.* **220** 286–297.

Gandois L, Agnan Y, Leblond S, Séjalon-Delmas N, Le Roux G and Probst A 2014 Use of geochemical signatures, including rare earth elements, in mosses and lichens to assess spatial integration and the influence of forest environment; *Atmos. Environ.* **95** 96–104.

Getty S R, Gutzler D S, Asmerom Y, Shearer C K and Free S J 1999 Chemical signals of epiphytic lichens in southwestern North America; natural versus man-made sources for airborne particulates; *Atmos. Environ.* **33** 5095–5104.

Gibson M D, Heal M R, Li Z, Kuchta J, King G H, Hayes A and Lambert S 2013 The spatial and seasonal variation of nitrogen dioxide and sulfur dioxide in Cape Breton Highlands National Park, Canada, and the association with lichen abundance; *Atmos. Environ.* **64** 303–311.

Göb S, Loges A, Nolde N, Bau M, Berner Z, Jacob D and Markl G 2013 Major and trace element compositions (including REE) of mineral, thermal, mine and surface waters in SW Germany and implications for water-rock interaction; *Appl. Geochem.* **33** 127–152.

Hathorne E C, Haley B, Stichel T, Grasse P, Zieringer M and Frank M 2012 Online preconcentration ICP-MS analysis of rare earth elements in seawater; *Geochem. Geophys. Geosyst.* **13** Q01020, https://doi.org/10.1029/2011GC003907.

Hathorne E C, Stichel T, Brück B and Frank M 2015 Rare earth element distribution in the Atlantic sector of the Southern Ocean: The balance between particle scavenging and vertical supply; *Mar. Chem.* **177** 157–171.

Hongo Y, Obata H, Alibo D S and Nozaki Y 2006 Spatial variations of rare earth elements in north Pacific surface water; *J. Oceanogr.* **62** 441–455.

Hsu S C, Liu S C, Jeng W L, Chou C C K, Hsu R T, Huang Y T and Chen Y W 2006 Lead isotope ratios in ambient aerosols from Taipei, Taiwan: Identifying long-range transport of airborne Pb from the Yangtze Delta; *Atmos. Environ.* **40** 5393–5404.

Kao S Y, Lu H Y, Liou T S, Chen W F, Chang P Y and Hsieh P S 2017 Study of diel hydrochemical variation in a volcanic watershed using principal component analysis: Tatun Volcano Group, North Taiwan; *Environ. Earth Sci.* **76** 193.

Komárek M, Ettler V, Chrastný V and Mihaljevič M 2008 Lead isotopes in environmental sciences: A review; *Environ. Int.* **34** 562–577.

Kousehlar M and Widom E 2020 Identifying the sources of air pollution in an urban-industrial setting by lichen biomonitoring – A multi-tracer approach; *Appl. Geochem.* **121** 104695.

Koz B, Celik N and Cevik U 2010 Biomonitoring of heavy metals by epiphytic lichen species in Black Sea region of Turkey; *Ecol. Indic.* **10** 762–765.

LeGalley E, Widom E, Krekeler P S M and Kuentz D C 2013 Chemical and lead isotope constraints on sources of metal pollution in street sediment and lichens in southwest Ohio; *Appl. Geochem.* **32** 195–203.

Leonardo L, Mazzilli B P, Damatto S R, Saiki M and Barros De Oliveira S M 2011 Assessment of atmospheric pollution in the vicinity of a tin and lead industry using lichen species *Canoparmelia texana*; *J. Environ. Radioact.* **102** 906–910.

Lin C H 2016 Evidence for a magma reservoir beneath the Taipei metropolis of Taiwan from both S-wave shadows and P-wave delays; *Sci. Rep.* **6** 39500.

Loppi S and Pirintsos S A 2003 Epiphytic lichens as sentinels for heavy metal pollution at forest ecosystems (central Italy); *Environ. Pollut.* **121** 327–332.

Lu H Y 2014 Application of water chemistry as a hydrological tracer in a volcano catchment area: A case study of the Tatun Volcano Group, North Taiwan; *J. Hydrol.* **511** 825–837.

Mezhibor A M, Bolshunova T S and Rikhvanov L P 2016 Geochemical features of sphagnum mosses and epiphytic lichens in oil and gas exploitation areas (the case of Western Siberia, Russia); *Environ. Earth Sci.* **75** 1260.

Nash T H 2008 *Lichen Biology*; Cambridge University Press, New York.

Nash T H and Gries C 2002 Lichens as bioindicators of sulfur dioxide; *Symbiosis* **33** 1–21.

Ndlovu N, Frontasyeva M, Newman R and Maleka P 2019 Moss and lichen biomonitoring of atmospheric pollution in the Western Cape Province (South Africa); *Am. J. Anal. Chem.* **10** 86–102.

Nesbitt H W 1979 Mobility and fractionation of rare earth elements during weathering of a granodiorite; *Nature* **279** 206–210.

Olivarez A M and Owen R M 1991 The europium anomaly of seawater: Implications for fluvial versus hydrothermal REE inputs to the oceans; *Chem. Geol.* **92** 317–328.

Paoli L, Vannini A, Monaci F and Loppi S 2018 Competition between heavy metal ions for binding sites in lichens: Implications for biomonitoring studies; *Chemosphere* **199** 655–660.

Parviainen A, Casares-Porcel M, Marchesi C and Garrido C J 2019 Lichens as a spatial record of metal air pollution in the industrialized city of Huelva (SW Spain); *Environ. Pollut.* **253** 918–929.

Piepgras D J and Jacobsen S B 1992 The behavior of rare earth elements in seawater: Precise determination of variations in the North Pacific water column; *Geochim. Cosmochim. Acta* **56** 1851–1862.

Prudêncio M I 2007 Biogeochemistry of trace and major elements in a surface environment (volcanic rock, soil, mosses, lichens) in the S. Miguel Island, Azores, Portugal; *J. Radioanal. Nucl. Chem.* **271** 431–437.

Purvis O W, Chimonides P D J, Jeffries T E, Jones G C, Rusu A M and Read H 2007 Multi-element composition of historical lichen collections and bark samples, indicators of changing atmospheric conditions; *Atmos. Environ.* **41** 72–80.

Purvis O W and Pawlik-Skowrońska B 2008 Chapter 12 Lichens and metals; In: *Stress in Yeast and Filamentous Fungi* (eds) Simon V A, Malcolm S and Pieter V W, Academic Press, London, pp. 175–200.

Rossbach M, Jayasekera U R, Kniewald G and Thang N H 1999 Large scale air monitoring: Lichen vs. air particulate matter analysis; *Sci. Total Environ.* **232** 59–66.

Sahu L K, Kondo Y, Miyazaki Y, Pongkiatkul P and Kim Oanh N T 2011 Seasonal and diurnal variations of black carbon and organic carbon aerosols in Bangkok; *J. Geophys. Res. Atmos.* **116** D15302.

Scholz F and Kahlert H 2015 The calculation of the solubility of metal hydroxides, oxide-hydroxides, and oxides, and their visualisation in logarithmic diagrams; *ChemTexts* **1** 7.

Seto M and Akagi T 2008 Chemical condition for the appearance of a negative Ce anomaly in stream waters and groundwaters; *Geochem. J.* **42** 371–380.

Shellnutt J, Belousov A, Belousova M, Wang K L and Zellmer G 2014 Generation of calc-alkaline andesite of the Tatun volcanic group (Taiwan) within an extensional environment by crystal fractionation; *Int. Geol. Rev.* **56** 1156–1171.

Sinha P R, Nagendra N, Manchanda R K, Ojha D K, Suneel Kumar B, Koli S K, Trivedi D B, Lodha R K, Sahu L K and Sreenivasan S 2019 Development of balloon-borne Impactor payload for profiling free tropospheric aerosol; *Aerosol. Sci. Technol.* **53** 231–243.

Stille P, Pierret M-C, Steinmann M, Chabaux F, Boutin R and Aubert D 2009 Impact of atmospheric deposition, biogeochemical cycling and water–mineral interaction on REE fractionation in acidic surface soils and soil water (the Strengbach case); *Chem. Geol.* **264** 173–186.

Symphonia K T and Nathan D S 2018 Geochemistry and distribution of sediments in the East Indian shelf, SW Bay of Bengal: Implications on weathering, transport and depositional environment; *J. Earth Syst. Sci.* **127** 96.

Taylor S R and McLennan S M 1985 *The continental Crust: Its Composition and Evolution*; Blackwell, Oxford.

Varrica D, Aiuppa A and Dongarrà G 2000 Volcanic and anthropogenic contribution to heavy metal content in lichens from Mt. Etna and Vulcano island (Sicily); *Environ. Pollut.* **108** 153–162.

Vázquez-Ortega A, Perdrial J, Harpold A, Zapata-Ríos X, Rasmussen C, McIntosh J, Schaap M, Pelletier J D, Brooks P D, Amistadi M K and Chorover J 2015 Rare earth elements as reactive tracers of biogeochemical weathering in forested rhyolitic terrain; *Chem. Geol.* **391** 19–32.

Veron A J, Church T M, Patterson C C and Flegal A R 1994 Use of stable lead isotopes to characterize the sources of anthropogenic lead in north Atlantic surface waters; *Geochim. Cosmochim. Acta* **58** 3199–3206.

Wang K L, Chung S L, Chen C-H, Shinjo R, Yang T F and Chen C H 1999 Post-collisional magmatism around northern Taiwan and its relation with opening of the Okinawa Trough; *Tectonophys.* **308** 363–376.

Wang K L, Chung S L, O'Reilly S Y, Sun S S, Shinjo R and Chen C-H 2004 Geochemical constraints for the genesis of post-collisional magmatism and the geodynamic evolution of the northern Taiwan region; *J. Petrol.* **5** 975–1011.

Weill D F and Drake M J 1973 Europium anomaly in plagioclase feldspar: Experimental results and semiquantitative model; *Science* **180** 1059–1060.

Will-Wolf S, Jovan S, Amacher M C and Patterson P L 2020 Lichen elemental indicators for air pollution in Eastern United States forests; a pilot study in the upper Midwest; General Technical Report PNW-GTR-985.Portland, Orogen: U.S. Department of Agriculture, Forest Service, Pacific Northwest Research Station, 178p.

Yao P H, Shyu G S, Chang Y F, Chou Y C, Shen C C, Chou C S and Chang T K 2015 Lead isotope characterization of petroleum fuels in Taipei, Taiwan; *Int. J. Environ. Res. Public Health* **12** 4602–4616.

Corresponding editor: N V Chalapathi Rao